FEDERAL UNIVERSITY OF UBERLÂNDIA

BIOTECHNOLOGY INSTITUTE

BIOTECHNOLOGY COURSE

VIRTUAL SCREENING OF POTENTIAL INHIBITORS AGAINST N-myristoyltransferase from *Plasmodium vivax*

Germano Yoneda Pereira Lima

Prof. Dr. Nilson Nicolau Junior

Biotechnology Institute

Uberlândia

December/2018

FEDERAL UNIVERSITY OF UBERLÂNDIA

BIOTECHNOLOGY INSTITUTE

BIOTECHNOLOGY COURSE

VIRTUAL SCREENING OF POTENTIAL INHIBITORS AGAINST N-myristoyltransferase from *Plasmodium vivax*

> Monograph presented as requirement for approval in the subject Completion of Coursework II, of Biotechnology's bachelor curse of Federal University of Uberlândia under guidance of Prof.Dr. Nilson Nicolau Junior
>
> Homologated by Biotechnology coordination course in __/__/____
>
>
> Prof. Dr. Edgar Silveira Campos

Uberlândia

December/2018

Federal University of Uberlandia
Institute of Biotechnology
Biotechnology Course

VIRTUAL SCREENING OF POTENTIAL INHIBITORS AGAINST N-myristoyltransferase from *Plasmodium vivax*

Germano Yoneda Pereira Lima

Approved by the Examination Board in: / /   Grade: ____

Name and signature from the Examination Board president

Uberlândia, 10 December 2018

Federal University of Uberlandia
Institute of Biotechnology
Biotechnology Course

VIRTUAL SCREENING OF POTENTIAL INHIBITORS AGAINST N-
myristoyltransferase from *Plasmodium vivax*

Germano Yoneda Pereira Lima

Prof. Dr. Nilson Nicolau Junior

Institute of Biotechnology

Homologated by Biotechnology
coordination course in __/__/____

Coordinator: Prof. Dr. Edgar Silveira Campos

Uberlândia, 10 December 2018

I dedicate this work to my parents, siblings and uncles, who provided me with everything I needed during my graduation.

Dedico este trabalho aos meus pais, irmãos e tios, os quais me proporcionaram tudo o que era necessário durante minha graduação.

List of Abbreviations and Acronyms

NMT - *N*-myristoyltransferase

CADD - Computer-Aided Drug Design

HsNMT1 - *Homo sapiens N*-myristoyltransferase 1

HsNMT2 - *Homo sapiens N*-myristoyltransferase 2

PvNMT – *Plasmodium vivax N*-myristoyltransferase

PfNMT – *Plasmodium falciparum N*-myristoyltransferase

ZDD – Natural drugs library extracted from ZINC

EXP – Drug likeness chemical compounds extracted from ChemBridge

DUD-E – Database of Useful Decoys: Enhanced

FRED – Docking software

PKCSM - predicting small-molecule pharmacokinetic properties using graph-based signatures

hERG - human Ether-à-go-go-Related Gene

AUC – Area under the curve

ABSTRACT:

Malaria is a tropical disease caused by parasites from *Plasmodium vivax*, which are normally associated with *Anopheles* spp. In 2016, an estimated 216 million cases occurred worldwide, causing 445 000 deaths. *N*-myristoyltransferase (NMT) is a very important enzyme related with the transfer of myristate acid from myristoyl coenzyme A to specific proteins in the glycine N-terminal residue, this process occurs at the same time of the translation, for this, aminopeptidases withdraw the initial methionine, making glycine the N-terminal amino acid. NMT inhibition demonstrated to leads parasite to cell death. To predict new potential inhibitors against NMT *Plasmodium*, Computer-Aided Drug Design (CADD) tools were used to alignment of pharmacophores, virtual screening, validation, docking and molecular dynamics.

Key words: *Plasmodium, N*-myristoyltransferase, Bioinformatics.

Summary

1. INTRODUCTION:

1.1 Malaria

Malaria is a tropical disease caused by parasites from *Plasmodium vivax*, which are normally associated with *Anopheles* spp. After the mosquito bite, the parasite shows the capacity to reach the liver and multiply quickly infecting erythrocytes after incubation period, which can range between 8 and 30 days causing serious symptoms such as: muscle and abdominal pain, fever, fatigue, nausea and diarrhea, tremors and vomiting. These parasite can also be transmitted through blood transfusions, transplants or by sharing contaminated syringes (ANVISA, 2008).

In 2016, an estimated 216 million cases occurred worldwide, of these cases 445 000 deaths, and an estimated US$ 2.7 billion was spent to control and elimination of malaria in endemic places, like Africa, which approximately 90% of malaria cases in 2016 occurred. The number of reported malaria cases in Brazil has decreased from 423,000 cases in 2010 to 157,100 in 2016 and the number of deaths has decreased from 76 cases in 2010 to 37 in 2016 (WHO, 2017).

The first records of malaria date back to 2.700 b.C. with the mention of prolonged fevers and melancholies. Described by the Canon of Chinese medicine, Nei Ching. The disease has been described over the centuries by numerous historical figures like: Plato, Homer and Shakespeare, being that Hippocrates was the first to do the connection between proximity to standing water and the incidence of fever in population. The word malaria comes from Italian origin (mal'aria) because in the XIV century there was a belief that the disease was transmitted by marshes and contained air (FRANÇA; DOS SANTOS; FIGUEROA-VILLAR, 2008).

One of the most important cases of malaria was registered in 1638, when the Countess of Chinchón was afflicted with a strong "terçan" fever. The Indians medicated her with a mixture of herbs called "quina-quina", which resulted in the cessation of fever and the cure.

The Jesuit priests of the Spanish mission eventually took with them the powder that had been used to produce the potion by the natives, which became known as the "Jesuit powder" presenting Quinone's, the first known treatment against the parasite (DE OLIVEIRA; SZCZERBOWSKI, 2009)

The drugs resistance has been one of the major problems in the treatment issue, since the administration of only one drug favors selective pressures selecting the resistant mutant parasites. Thus, the literature suggests that the use of drugs cocktails reduce the probability of emergence of resistant strains (HASTINGS; DONNELLY, 2005).

The gold standard of malaria treatment consists in artemisinin and Synthetic derivatives, but this treatment has shown a loss of efficiency (DAS et al., 2009).

1.2 *N*-myristoyltransferase and motivation

With the artemisinin loss of efficacy new drugs with different mechanisms of action have been sought, such as the inhibition of *N*-myristoyltransferase (NMT)(YU et al., 2012).

N-myristoyltransferase (NMT) is a very important enzyme in eukaryotes, highly conserved structure among species, however inhibitors of this enzyme may be selective for Plasmodium due to the ability of *Homo sapiens N*-myristoyltransferase 1(HsNMT1) to tolerate conformational changes, besides, the overexpression of HsNMT1 and HsNMT2 has been shown to be related to carcinomas and viral replication. (TATE et al., 2014). The NMT catalyzes a bi-bi mechanism: The covalent transfer of myristate acid from myristoyl coenzyme A to specific proteins such tyrosine kinases, G-proteins, and other heterodimer proteins, in the glycine N-terminal residue, this process occurs at the same time of the translation, for this, aminopeptidases withdraw the initial methionine, making glycine the N-terminal amino acid (Figure 1) (WRIGHT et al., 2010; ZHAO; MA, 2014).
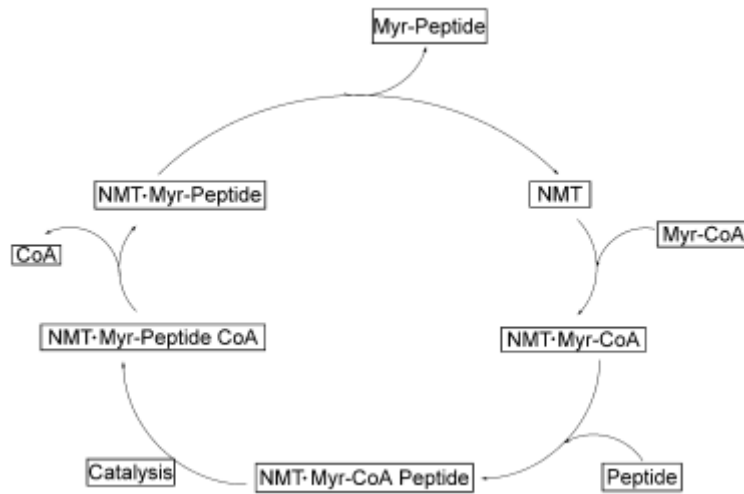
Figure 1-Bi-Bi mechanism of NMT catalytic cycle (ZHAO; MA, 2014).

NMT inhibition induces parasite cell death, since the myristylation is involved with regulation of protein complex and stability (WRIGHT et al., 2014). Besides, NMT showed to be important in signaling pathway in mice during the early development (YANG et al., 2005).

NMT was described for the first time in 1987, in *Saccharomyces cerevisiae*(TOWLER et al., 1987). In 2000 the first isolation of NMT from *Plasmodium* spp. has been shown, curiously it had only one form, differently to all metazoan, which exhibit two isoforms of this enzyme (TATE et al., 2014).

NMT is also expressed in humans, which could be a hindrance however according to (YU et al., 2012) the residue Y296 is the key to the selectivity between *Homo sapiens* NMT and PvNMT caused by the interaction Y296 and inhibitor.

The motivation of this work is to provide a new potential target to treat malaria, since chloroquine has lost efficacy and artemisinin compounds has shown an emerging resistance against *Plasmodium falciparum* and *vivax* (DAS et al., 2009).

1.3 Computer-Aided Drug Design

For a new drug to reach the market a lot of bench test are required, which require long time frames and resources, thereat arises the need to use bioinformatics tools that permit to realize a filter in the bench tested compounds, increasing the efficiency and efficacy of the method, this methodology is called Computer-Aided Drug Design (ACDD), which aim to determine interatomic distance, electronic densities, evaluating the conformational equilibrium of the molecules and their minimum energy, Allowing to evaluate specific interactions of the drugs based on pharmacophores points, which were described at the first time by Ehrlich in 1909 as a molecular structure that carries essential characteristics for biological activity, this definition was updated in 1998 by IUPAC for a set of steric and electronic characteristics necessary to ensure optimal supramolecular interactions with a specify biological agent and to trigger or block their biological response. (BARREIRO et al., 1997; EHRLICH, 1909; OOMS, 2000; WERMUTH et al., 1998).

2.OBJECTIVES:

2.1 General objective

Predict potential ligands against PvNMT using known compounds libraries and bioinformatics tools.

2.2 Specific objectives

- Perform an alignment with known inhibitors against NMT vivax.

- Create a shape-based model based on the alignment of the ligand.

- Create potential decoys using known inhibitors.

- Perform a shape-based model validation.

- Perform a virtual screening using known libraries.

- Perform molecular docking of the best ligands.

- Selection of the best ligand according to the toxicity parameters.

- Simulate molecular dynamics of the best complexes

- Evaluate the protein-ligand in interactions.

3.MATERIAL AND METHODS:

3.1 Getting NMT, inhibitors and libraries

The known protein-ligand complex structures of NMT from *P. vivax* were retrieved from Protein Data Bank (PDB). Six PBD protein-inhibitors complexes were chosen: 4B12, 4B13, 4B14, 4BBH, 4CAE and 4CAF. *Plasmodium vivax* NMT (PvNMT) structures were used due to absence of *Plasmodium falciparum* (PfNMT) crystallography in 2016 . According to Yu et al., (2012) PvNMT shares 81% identity of the sequence with PfNMT, which suggests that PvNMT can be used as model to PfNMT. The compound libraries used on the virtual screening were retrieved from ZINC (IRWIN; SHOICHET, 2005) and Chembridge (Corporation, San Diego, California) Databases. Two subsets, ZDD, a library of commercially available approved drugs from ZINC and EXP, a stringent library of druglike compounds from Chembridge were used.

3.2 Getting shape-based model

PharmaGist webserver (DROR et al., 2009) was used to provide a pharmacophore alignment using known inhibitors against NMT extracted from PDB complexes 4B12, 4B13, 4B14, 4BBH, 4CAE and 4CAF. Alignments with the best pharmagist score were submitted to vRocs(HAWKINS; SKILLMAN; NICHOLLS, 2007), to create shape-based models

3.3 Model validation

In order to validate the shape-based models known inhibitors based on Bell et al (2012) were used. The inhibitors used are indicated in the Table 1, all 10 structures were design using PubChem Draw Structure (KIM et al., 2016) in SMILES format.

Table 1-SMILES format of known inhibitors against NMT.

C1=CC=C(C(=C1)C(=O)N([C@H]2CN(CC2)C(CN(C)C)=O)[H])C(F)(F)F
C1=C(C=C(C=C1C2CCN(CC2)CC4=NC3=CC(=CC=C3[N]4C)C)F)F
C1=CC=CC(C1C)C2=CCC3C(=C2)C(=NN3C)CN(C)C
C1(=CC(=C(C=C1)CN(C(=O)C2CN(C2)C3=C(C=NC(=N3)N(CCN(C)C)C)Cl)[H])F)F
N(C(=O)C1CN(C1)C2=C(C=NC(=N2)N(CCN(C)C)[H])Cl)(CC3=NC=C(N=C3)C)[H]
C1=C(C=CC=N1)CCN(CC2=CC(=CC=C2)C3=CC=CC(=C3)CN4CC5C(CC4)N=CS5)[H]
C1=CC(=CC=C1[C@@H]2[C@H](CN(C2)C(C[C@@H](CC3=CC=C(C=C3)Cl)N([H])[H])=O)CO[H])CC
C1CC(CCN1C)N(C)C2=NC3=C(C(=N2)N(CCC#C)C)SC(=C3)C
C1C(CCN(C1)[H])C2=C[N](C3=C2C=C(C=C3)N(C(CC4=CC=C(C=C4)F)=O)[H])[H]
C1=CC(=CC=C1)Cl.C2[C@H](CN(C2)C(C[C@@H](CC3=CC=C(C=C3)Cl)N([H])[H])=O)CO[H]

DUD-E webtool (MYSINGER et al., 2012) was used to predict decoys using known inhibitors (Table 1), decoys are structures that have similar proprieties with ligand but different chemical structure. To perform the validation using shape-based models, decoys (compounds that can bind but have no response) and actives structures were submitted to a comparative virtual screening. Previously actives and decoys were prepared using QUACPAC (OpenEye Scientific Software, Santa Fe, NM. http://www.eyesopen.com) to generate tautomer's and to

protonate ligand states to physiological pH 7.4. Besides, Omega (HAWKINS et al., 2010) was used to generate 3D bioactive conformers for each molecule

3.4 Libraries preparation.

The EXP is a library extracted from ChemBrigde, which have chemical compounds with drug likeness proprieties. ZDD library was extracted from ZINC and have natural compounds that are already drugs.

In active and ligand preparation step the EXP and ZDD were prepared using QUACPAC. Further Omega (HAWKINS et al., 2010) were used in order to filter compounds with druglike features and generate 3D conformers for each molecule.

3.5 Virtual Screening and docking.

Virtual screening using shape-based model were performed on vROCS. The best 500 compounds were selected using *Tanimoto combo score*. In the next step a molecular docking was performed between NMT and 500 best compounds using FRED (MCGANN, 2011).

3.6 Pharmacokinetics

Pharmacokinetics analysis were analyzed using PKCSM (PIRES; BLUNDELL; ASCHER, 2015), a machine-learn platform, which relies on distance/pharmacophore patterns encoded as graph-based signature. In this work was choose some toxicity parameters, such as: AMES toxicity, Max tolerated dose (human), hERG I inhibitor, hERG II inhibitor, Oral Rate Acute Toxicity (LD50), Oral Rat Chronic Toxicity (LOAEL), Hepatotoxicity and Minnow toxicity.

The AMES toxicity parameter is used to predict a potential mutagenic compound using in bacteria, so if the test is positive, it shows that the compound in question is mutagenic.

The Maximum Tolerated Dose (human) parameter estimate the toxic dose threshold of chemical in humans (mg/kg/day), being less or equal to 0.477 (mg/kg/day) considered as low and high if greater than 0.477 (mg/kg/day).

The hERG I parameter analyses higher risks to develop the long QT syndrome (LQTS) in human, which is a heart rhythm disorder that can cause chaotic and rapid heartbeat. It tests if it generates an inhibition of the potassium channels, altering the heartbeat frequency and order.

The Oral Rate Acute Toxicity (LD50) is the lethal dosage values that is necessary to cause the death of 50% of a group of tests

The Oral Rat Chronic Toxicity refers to identify the lowest dose of compound that results in an observed adverse effect (LOAEL).

The Hepatotoxicity parameters refers a liver associated side effects observed in humans, being able to cause or not.

The Minnow toxicity: the lethal concentration values (LC50) represent the concentration of a molecule necessary to cause the death of 50% of the Flathead Minnows.

Utilizing toxicity parameters was possible to select the best ligand in each library (EXP, ZDD) according to pharmacokinetics (Table 4).

3.7 Molecular Dynamics

The best compounds of each libraries, according to PKCSM parameters was submitted to molecular dynamics in complex of NMT. Topology and parameters for each ligand were performed using SwissParam (ZOETE et al., 2011), which uses CHARMM force field. The molecular dynamics were performed on GROMACS (ABRAHAM et al., 2015), using CHARMM27 force-field, water model chosen was TIP3P. The unit cell was defined as triclinic

shape, water and ions were added and energy minimization were performed using 10000 picoseconds.

3.8 Protein-ligand 2D interaction

Protein-ligand Interactions 2D diagrams were generate using LigPlot+(LASKOWSKI; SWINDELLS, 2011). Molecular dynamics frames 0 (first), 500(half) and 1000(last) were plotted to evaluate the protein-ligand interactions along time.

4. RESULTS AND DISCUTION

4.1 Alignment and Shape-based model

The best result of PharmaGist's alignment exhibited score 36.000 and 6 ligands (NMT inhibitors). Sixteen queries were generated from this alignment using vRocs (HAWKINS; SKILLMAN; NICHOLLS, 2007), The query models were edit manually and validate using AUC analysis (Table 2).

Table 2- All queries with the number of pharmacophoric points and area under curve(AUC)

Query/model number	Pharmacophore points	AUC
1	5	0.714
2	5	0.764
3	5	0.727
4	5	0.797
5	5	0.849
6	5	0.749
7	5	0.755
8	5	0.604
9	6	0.739
10	6	0.780
11	6	0.682
12	6	0.727
13*	6	0.880
14	6	0.842
15	6	0.845
16	6	0.743

*Best query according to AUC analysis

The chosen model was the number 13 (Figure 2), according the higher AUC (Figure 3), which means area under the curve, it is a simply probability that a randomly chosen active ligand instead of inactive ligand.
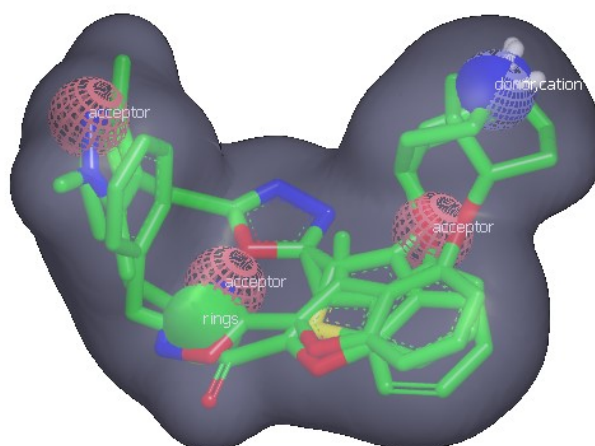

Figure 2- Shape based model Chosen with 6 pharmacophores points, 3 acceptors, 1 donor, 1 cation and one ring
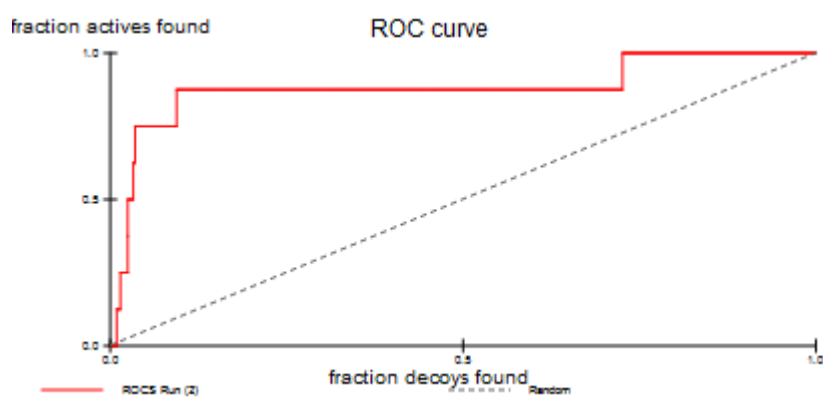

Figure 3- ROC curve obtained in the validation of the model. Dashed line indicates aleatory results, the red line indicated ROC curve generated, and all area under the curve indicated model accuracy.

4.2 Shape-based virtual screening and Docking

Virtual screening was performed using model 13 on vROCS and the libraries EXP and ZDD which are derived from ChemBridge and ZINC respectively. From each library virtual screening results in the best 500 compounds according to *tanimoto combo* score.

Screened libraries were submitted to protein ligand docking using FRED, the 1% best docked compounds according to *Chemgauss4* score were maintained, 8 ligands from EXP and 6 from ZDD. The best docked ligands were submitted to pharmacokinetics prediction analyses using PKCSM, which calculate proprieties, all-pair shortest paths and use a distance-based signature to predict the toxicity parameters (Table 3)
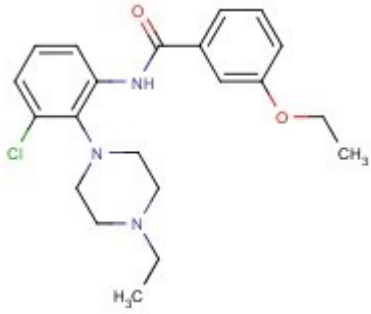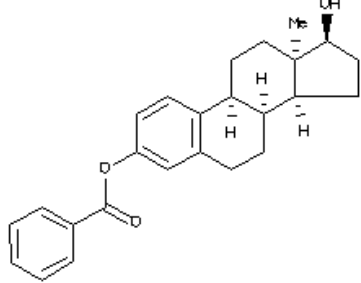
4.3 Toxicity Analysis.

The importance of toxicity analysis is to predict if the potential inhibitors presents the applicable parameters to drug selection, objectifying a future administration in human organism. The results were judged by positive/negative pharmacokinetic characteristics, in this work was choose some toxicity parameters, such as: AMES toxicity, Max tolerated dose (human), hERG I inhibitor, Oral Rate Acute Toxicity (LD50), Oral Rat Chronic Toxicity (LOAEL), Hepatotoxicity and Minnow toxicity (Table 3), selected ligands Exemplified (Table 4).

Table 3 - Potential toxicity of the best hits in each library, the squares in green shows best values while the red squares shows the worst values. Also, the yellow squares represent the intermediated values.

Código ChemBridge	AMES toxicity	Max, tolerated dose (human)	hERG I inhibitor	Oral Rat Acute Toxicity (LD50)	Oral Rat Chronic Toxicity (LOAEL)	Hepato toxicity	Minnow toxicity
9072821	Yes	-0.37	No	2.472	1.354	Yes	2.726
9235556	No	0.463	No	2.564	0.836	Yes	-0.054
5925531	No	-0.666	No	2.824	2.083	Yes	1.403
9223087	No	-0.225	No	2.464	0.971	Yes	3.469
5277870	Yes	-0.158	No	2.435	0.339	No	0.701
9063888	Yes	-0.343	No	2.674	0.979	Yes	4.338
9120471*	No	0.261	No	2.626	0.753	Yes	3.487
9112974	No	0.229	No	2.582	0.891	Yes	3.652
Código ZINC	AMES toxicity	Max, tolerated dose (human)	hERG I inhibitor	Oral Rat Acute Toxicity (LD50)	Oral Rat Chronic Toxicity (LOAEL)	Hepatotoxicity	Minnow toxicity
ZINC00968278	No	-0.524	No	2.263	1.606	No	1.392
ZINC00968278-2 (Tautômero)	No	-0.494	No	2.322	1.443	No	1.233
ZINC03830766*	No	0.017	No	2.794	2.136	No	-0.352
ZINC00968276	No	-0.524	No	2.263	1.606	No	1.392
ZINC12503187	Yes	0.37	No	2.71	1.296	Yes	1.257
ZINC00968276-2 (Tautômero)	No	-0.494	No	2.322	1.443	No	1.233

Table 4 -Selected ligand in each library

Library	Ligand(compound)	2D Structure
Exp	N-[3-chloro-2-(4-ethyl-1-piperazinyl)phenyl]-3-ethoxybenzamide ChemBridge: 9120471	
Zdd	17-hydroxyestra-1,3,5(10)-trien-3-yl benzoate ZINC03830766	

4.4 Molecular Dynamics Analysis

The prediction of root mean square deviation (RMSD), vacuum minimum energy and hydrogen bonds between protein and ligand were extracted from dynamics trajectory using specific tools from GROMACS analysis (ABRAHAM et al., 2015).

Estradiol analog (ZINC03830766) prediction showed a low and similar root-mean-square deviation (RMSD) to the known inhibitor extracted from the original (X25) NMT- ligand complex and NMT alone (PDB:4B13). Besides, low and stable RMSD results denotes protein-ligand complex stability along dynamics for each complex tested (Figure 4).
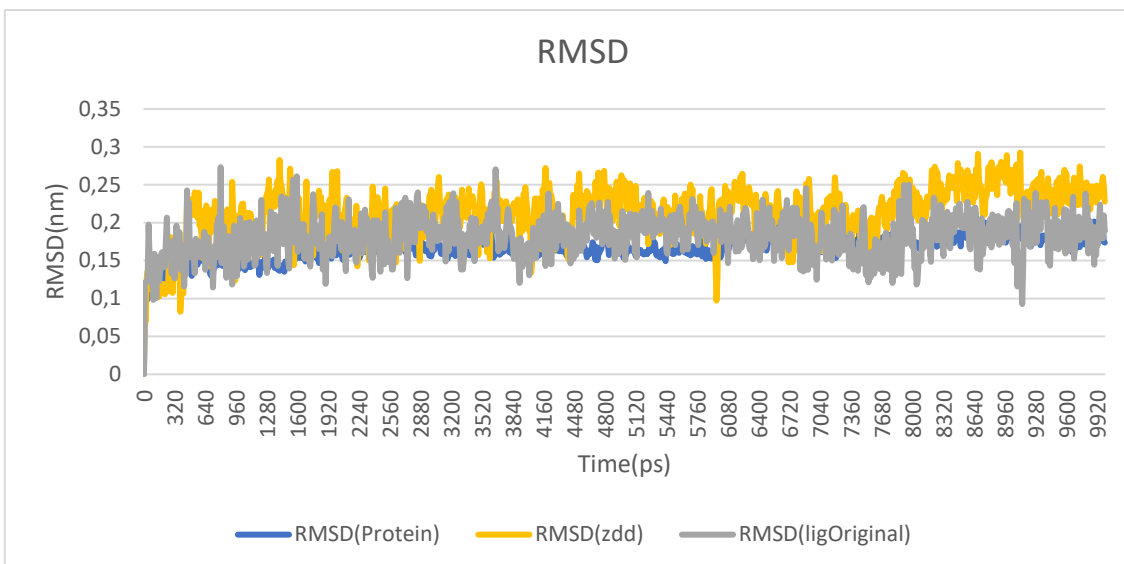
Figure 4 - Root mean square deviation in nanometers over the time for ZINC: 03830766 (yellow), X25 (gray) and only NMT(dark blue)

ZINC03830766-NMT complex featured a higher minimum energy (Figure 5), this fact can contribute for lower stability, but can be explained by the similarity with cholesterol structure, which has condensed chains with non-polar interactions which are more difficult to simulate (RÓG et al., 2009).
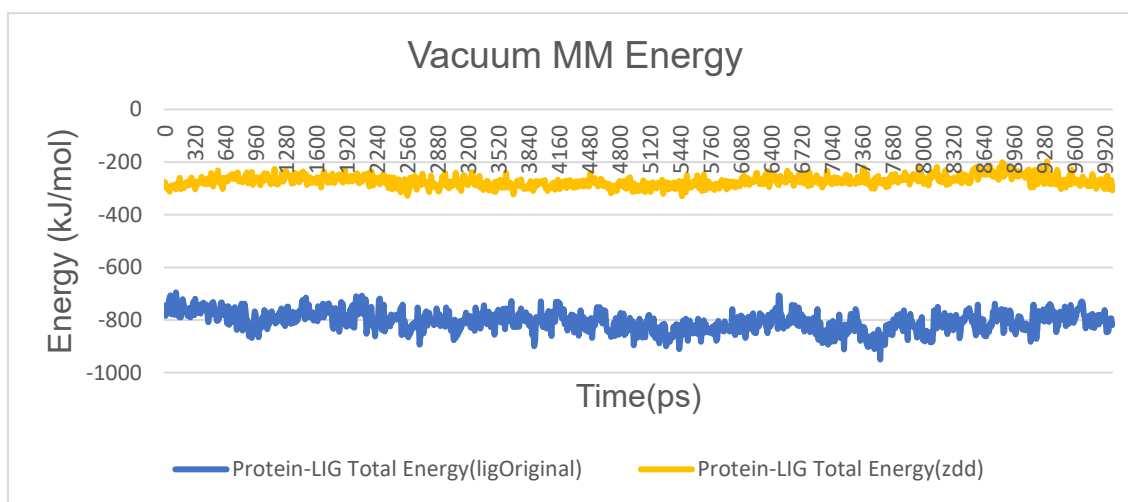

Figure 5 Energy(kJ/mol) over time (picoseconds) for X25 (blue) and ZINC:03830766 (Yellow)

ZINC03830766-NMT complex also exhibited a similar hydrogen bonds profile in comparison with X25-NMT complex, which indicates more similar interactions profile over time (Figures 6,7,11).
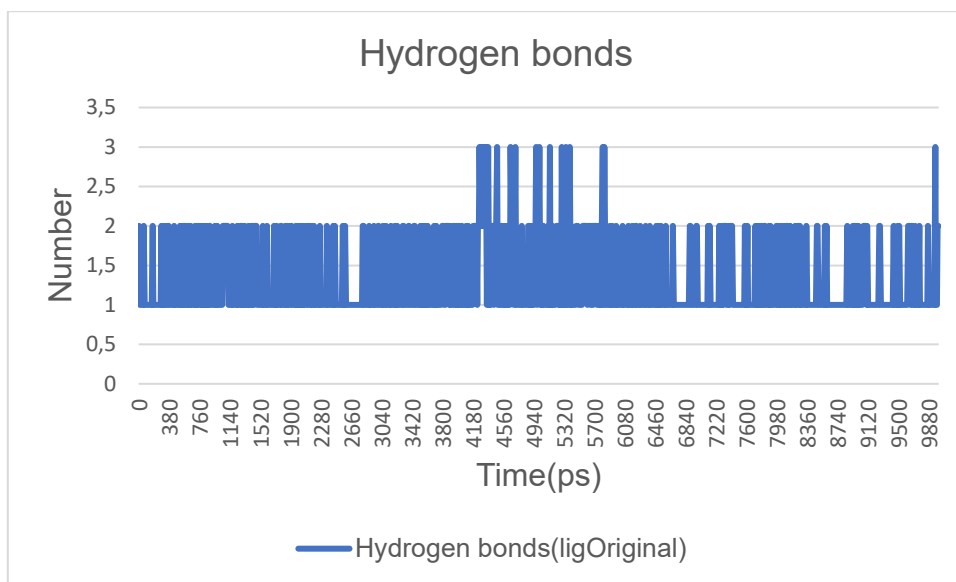

Figure 6- Number of Hydrogen bonds over the time (picoseconds) for X25
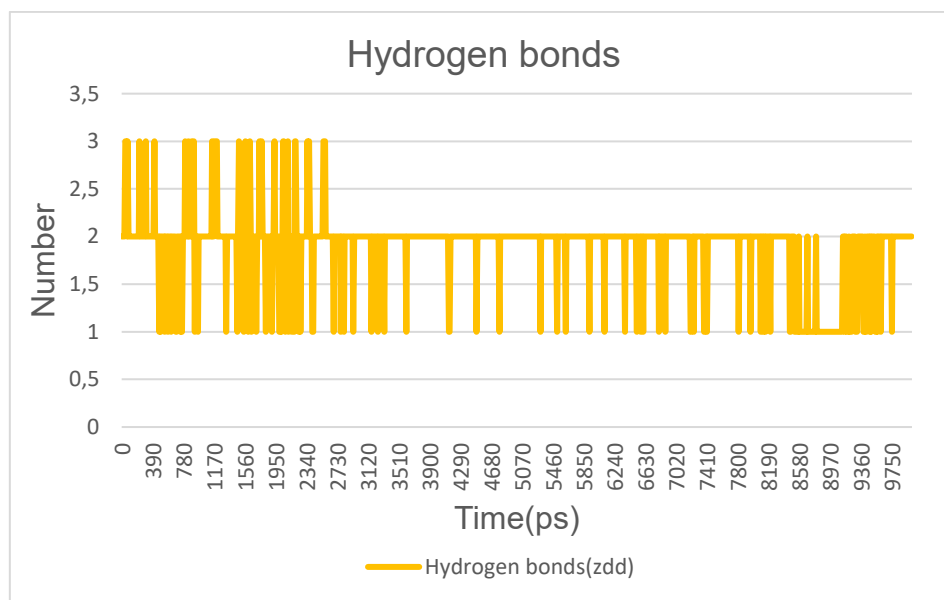

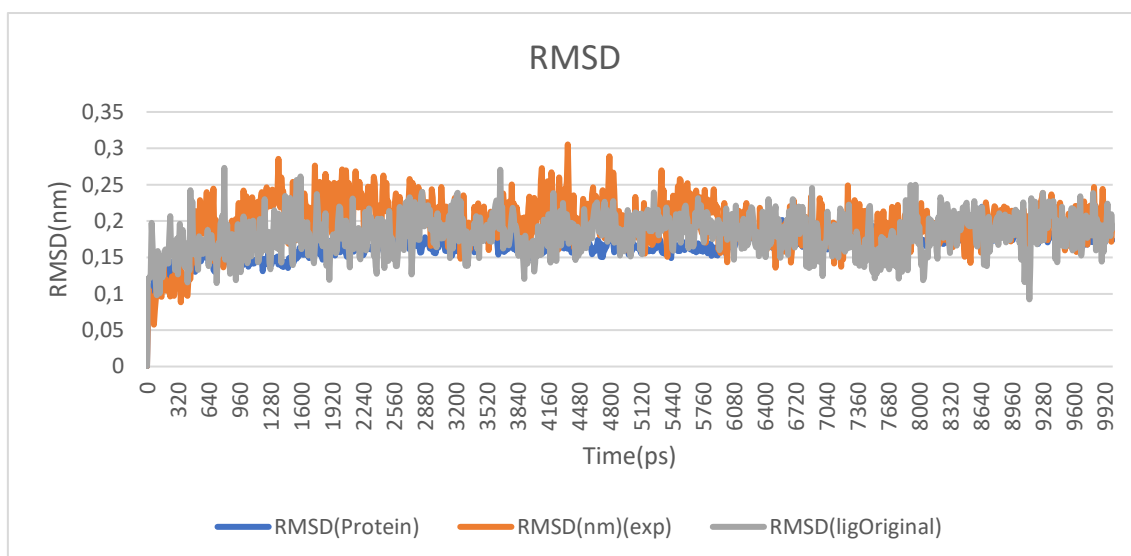Figure 7- Number of Hydrogen bonds over the time (picoseconds) for ZINC:03830766

Figure 8- Root mean square deviation in nanometers over the time for

ChemBridge:9120471 (orange) X25(gray) and only NMT(light blue)

ChemBridge Molecule 9120471 prediction showed a low and similar root-mean-square deviation (RMSD) to known inhibitor extracted from the original (X25) NMT-ligand complex and NMT alone (PDB:4B13). Besides, low and stable RMSD results denotes protein-ligand complex stability along dynamics for each complex tested (Figure 8).

The 9120471-NMT complex simulation showed a lower minimum energy (Figure 9), which can contribute to compound stability over time.
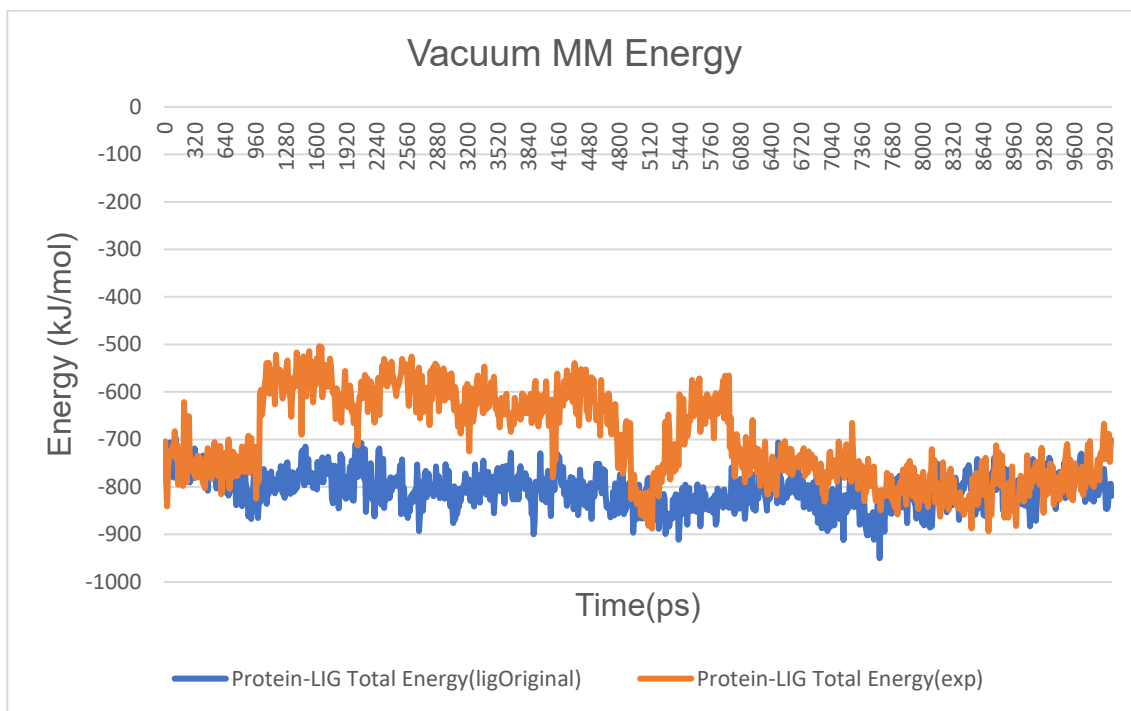

Figure 9- Energy(kJ/mol) over time(picoseconds) for X25(blue) and ChemBridge:9120471 (Orange)

Hydrogen bonds profile prediction (Figure 10) was discrepant for known ligand (Figure 6 and 11), this fact can show us a different profile of interaction over the time. However, in the last frames, the number of hydrogen bonds and the minimum energy are similar in both complexes 9120471-NMT and X25-NMT.
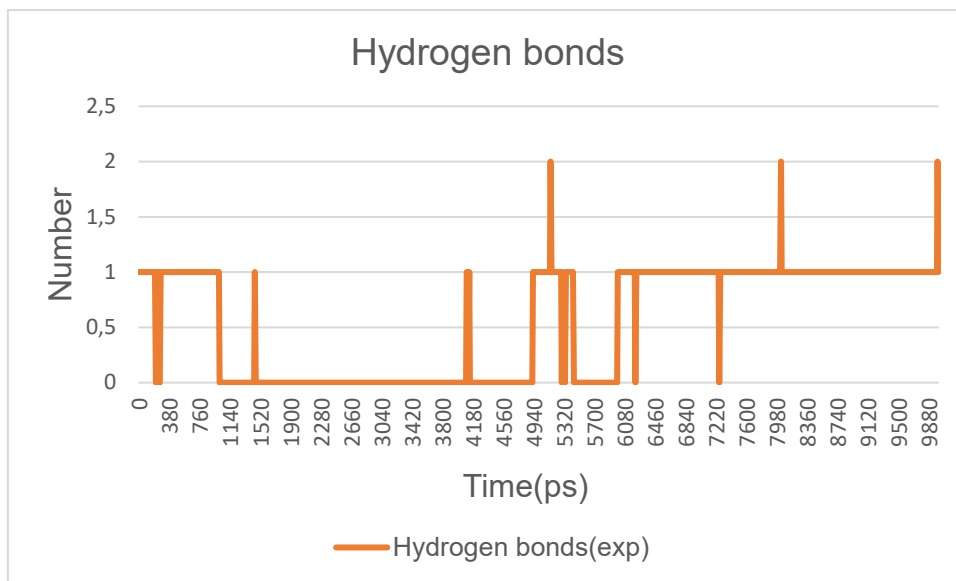
Figure 10- Number of Hydrogen bonds over the time (picoseconds) for
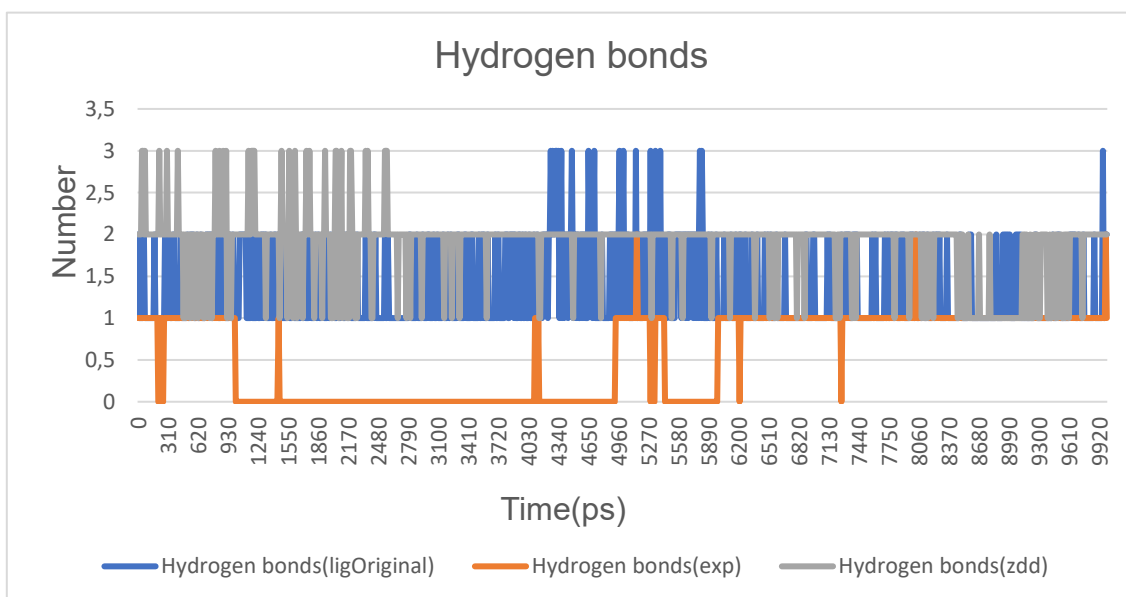
ChemBridge:9120471

Figure 11- Number of Hydrogen bonds over the time (picoseconds) for ZINC:03830766

(gray), ChemBridge:9120471 (orange) and X25 (blue)

4.5 2D Interaction protein-ligand and general discussion

In the 2D diagrams, the Figures 12,13,14 show the interaction between known

ligand over the dynamics frames 0,500 and 1000.The Figures 15,16,17 show the

interaction between EXP ligand over the dynamics frames 0,500,1000, and Figures

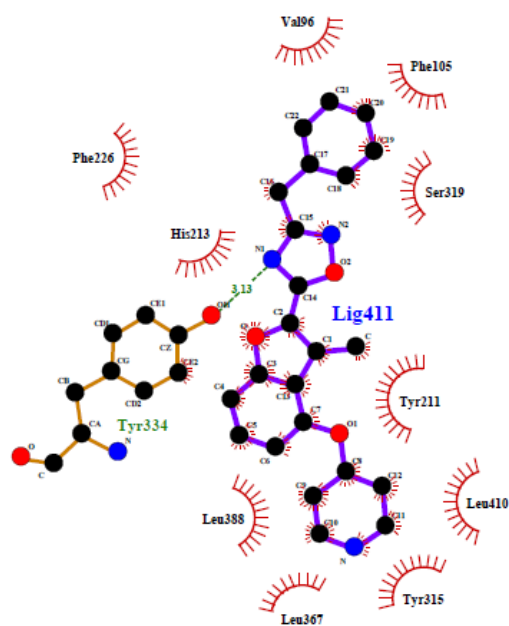18,19,20 show the interaction between ZDD ligand over the dynamics the frames 0,500,1000 respectively.

Figure 12- Frame 0: Interactions between NMT and X25, the ligand molecule is indicated in purple on the active site of the enzyme, the dark red shapes indicate hydrophobic interactions with amino acids residues, green dashed lines indicate hydrogen bonds, brown lines indicate non-ligand bonds and purple ligand bonds, black balls corresponding atoms involved in hydrophobic contact.

Figure 13- Frame 500: Interactions between NMT and X25, the ligand molecule is indicated in purple on the active site of the enzyme, the dark red shapes indicate hydrophobic interactions with amino acids residues, green dashed lines indicate hydrogen bonds, brown lines indicate non-ligand bonds and purple ligand bonds, black balls corresponding atoms involved in hydrophobic contact.
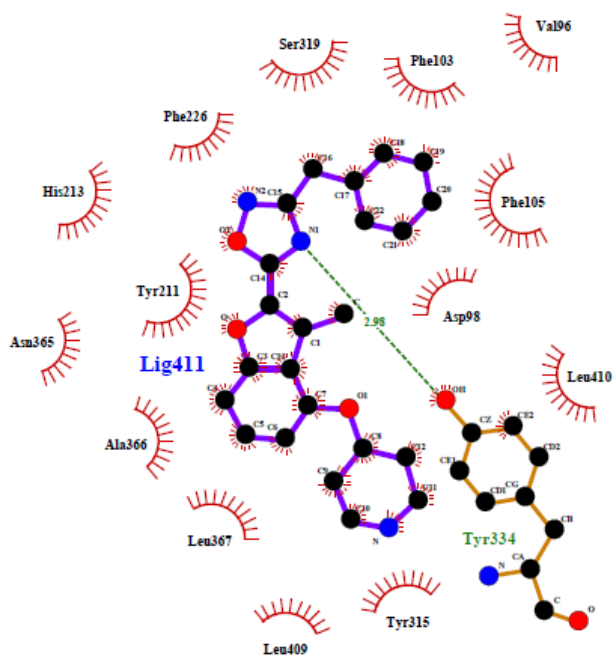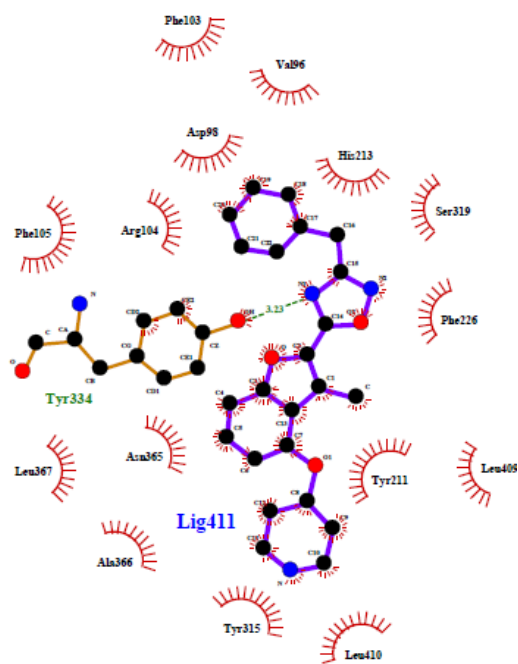
Figure 14- Frame 1000: Interactions between NMT and X25, the ligand molecule is indicated in purple on the active site of the enzyme, the dark red shapes indicate hydrophobic interactions with amino acids residues, green dashed lines indicate hydrogen bonds, brown lines indicate non-ligand bonds and purple ligand bonds, black balls corresponding atoms involved in hydrophobic contact.
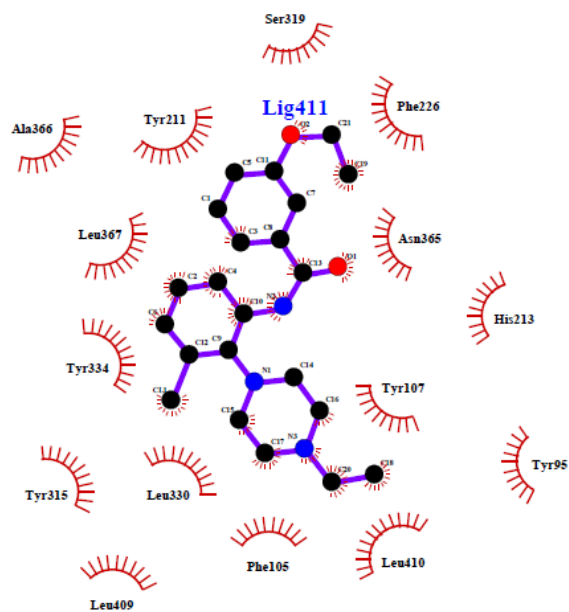
Figure 15 - Frame 0: Interaction between 9120471 and NMT, the ligand molecule is indicated in purple on the active site of the enzyme, the dark red shapes indicate hydrophobic interactions with amino acids residues, green dashed lines indicate hydrogen bonds, brown lines indicate non-ligand bonds and purple ligand bonds, black balls corresponding atoms involved in hydrophobic contact.

Figure 16 - Frame 500: Interaction between 9120471, the ligand molecule is indicated in purple on the active site of the enzyme, the dark red shapes indicate hydrophobic interactions with amino acids residues, green dashed lines indicate hydrogen bonds, brown lines indicate non-ligand bonds and purple ligand bonds, black balls corresponding atoms involved in hydrophobic contact.

Figure 17- Frame 1000: Interaction between 9120471, the ligand molecule is indicated in purple on the active site of the enzyme, the dark red shapes indicate hydrophobic interactions with amino acids residues, green dashed lines indicate hydrogen bonds, brown lines indicate non-ligand bonds and purple ligand bonds, black balls corresponding atoms involved in hydrophobic contact.
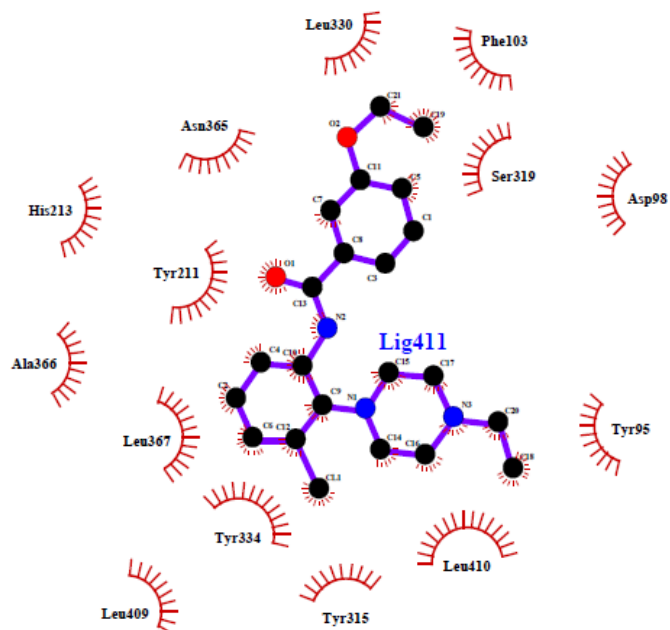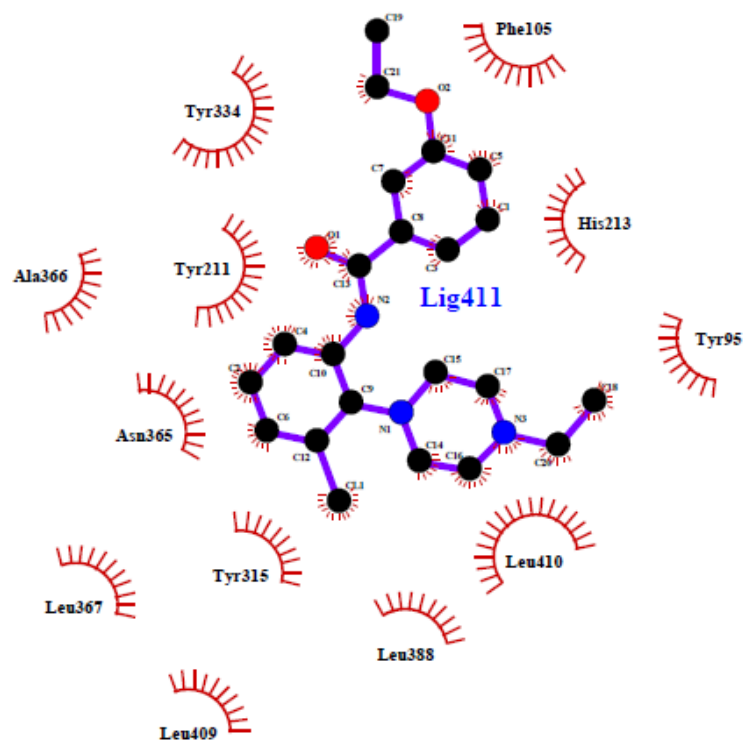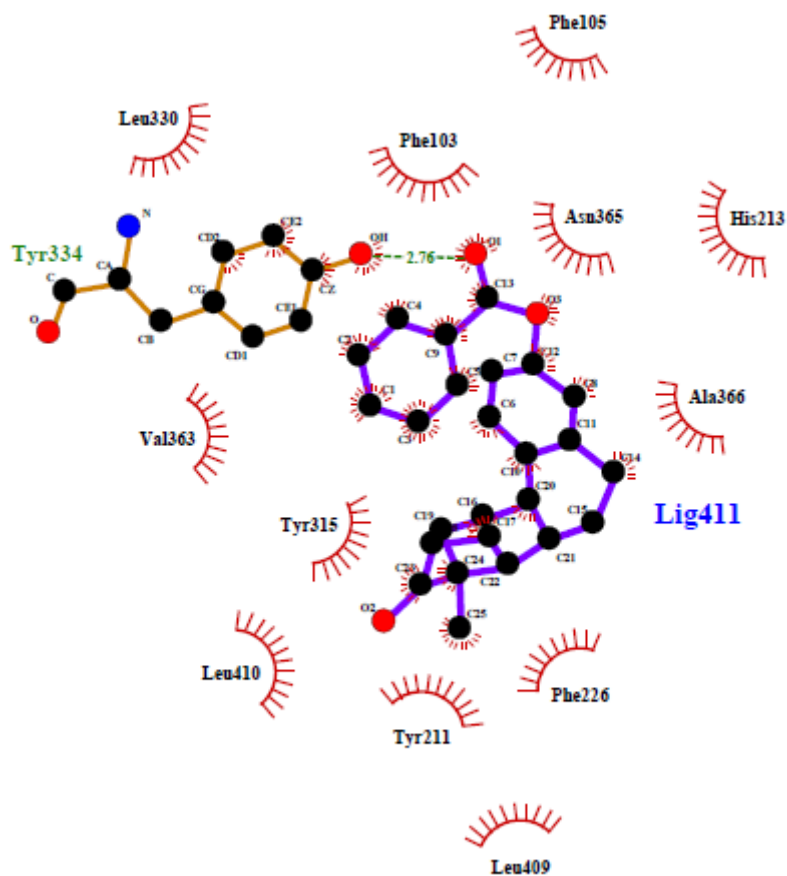
Figure 18- Frame 0: Interaction between ZINC03830766 and NMT, the ligand molecule is indicated in purple on the active site of the enzyme, the dark red shapes indicate hydrophobic interactions with amino acids residues, green dashed lines indicate hydrogen bonds, brown lines indicate non-ligand bonds and purple ligand bonds, black balls corresponding atoms involved in hydrophobic contact.
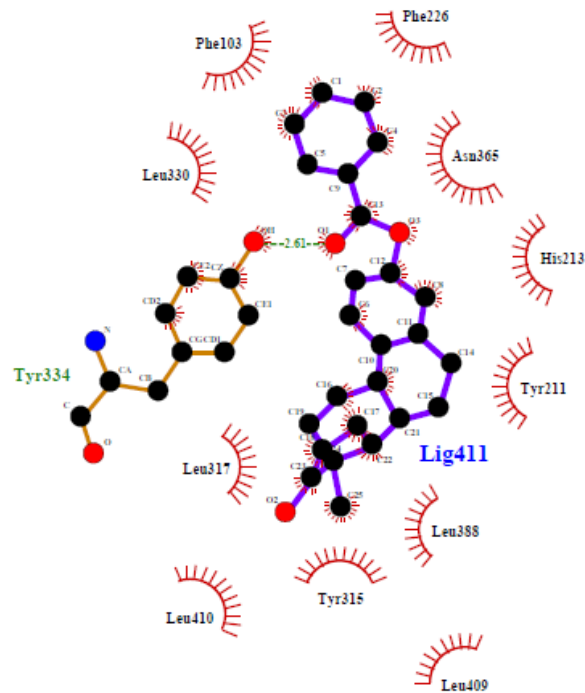
Figure 19- Frame 500: Interaction between ZINC03830766 and NMT, the ligand molecule is indicated in purple on the active site of the enzyme, the dark red shapes indicate hydrophobic interactions with amino acids residues, green dashed lines indicate hydrogen bonds, brown lines indicate non-ligand bonds and purple ligand bonds, black balls corresponding atoms involved in hydrophobic contact.

Figure 20-Frame 1000: Interaction between ZINC03830766 and NMT, the ligand molecule is indicated in purple on the active site of the enzyme, the dark red shapes indicate hydrophobic interactions with amino acids residues, green dashed lines indicate hydrogen bonds, brown lines indicate non-ligand bonds and purple ligand bonds, black balls corresponding atoms involved in hydrophobic contact.
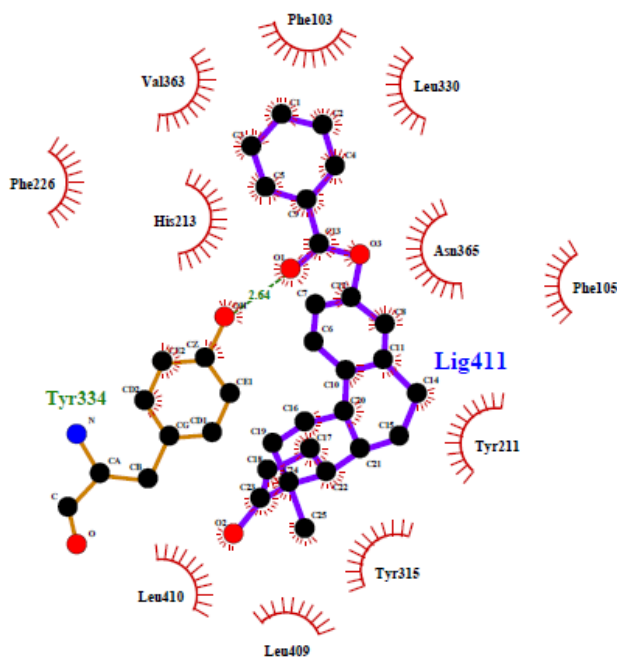
In the 2D diagrams is also possible to see that the ligand ZINC03830766 show a profile of interactions with the amino acids very similar to X25, mainly for the hydrogen bond with the Tyr334 in both cases. The most part of the interactions of non-ligand residues involved in hydrophobic contact is maintained for all ligands.

Estradiol and analogs showed already inhibition effect against protozoa influencing immune response, altering the response in a systemic pathway including innate immunity cells and adaptive immune response. Although the incidence of *Plasmodium* infections has not been intensively studied yet, females have been reported

a higher mortality rates even though the incidence between males and females seems the same. Pregnant women showed a greater risk than non-pregnant women, according to sex-hormones like estradiol, which can also create an immune response impairment (ROBERTS; WALKER; ALEXANDER, 2001). We hypothesize that estradiol and analogs though can potentially inhibit NMT and decreases parasite viability in an effective dose to inhibit the enzyme the systemic immune response is more prevalent. The systemic response showed to be more important than the inhibition of NMT, according to the estradiol levels in pregnant woman and the capacity of microbes to influence the hormones levels to improve their growth (VOM STEEG; KLEIN, 2017).

The other compound tested on molecular dynamics (*N-[3-chloro-2-(4-ethyl-1-piperazinyl) phenyl]-3-ethoxybenzamide*) (9120471) haven't been synthetized and tested yet, according to the chemical library information and literature.

5. CONCLUSION

In this work, we simulate microenvironments and the interaction between protein and potential-ligands for *Plasmodium vivax* NMT. This study used the concept of alignment of known inhibitors to create sixteen shape-based models, which were validated, and the best were chosen to virtual screening, which was used performed a virtual screening using chosen libraries. Then the docking protein-ligand aided in the search for the best ligands for NMT. Further we elected the best potential ligands according their pharmacokinetics. The molecular dynamics were performed then the energy of the interaction, hydrogens bond interactions, and root mean square deviation between protein-ligand were studied. Thus, we could have selected from several more than 50 thousand compounds two potentially stable ligands for PvNMT, one of them

potentially safe (ChemBridge9120471) and other one with effects not so well known, these will test in future experiments.

6. REFERENCES

ABRAHAM, M. J. et al. Gromacs: High performance molecular simulations through multi-level parallelism from laptops to supercomputers. **SoftwareX**, v. 1–2, p. 19–25, 2015.

ANVISA. Conheça a malária. **Conheça a malária**, p. 1–8, 2008.

BARREIRO, E. J. et al. Modelagem Molecular: Uma Ferramenta para o Planejamento Racional de Fármacos em Química Medicinal. **Química Nova**, v. 20, n. 3, p. 300–310, 1997.

BELL, A. S. et al. Selective inhibitors of protozoan protein N-myristoyltransferases as starting points for tropical disease medicinal chemistry programs. **PLoS Neglected Tropical Diseases**, v. 6, n. 4, 2012.

DAS, D. et al. Artemisinin Resistance in. **The new england journal of medicine**, v. 361, n. 5, p. 455–467, 2009.

DE OLIVEIRA, A. R. M.; SZCZERBOWSKI, D. Quinina: 470 anos de história, controvérsias e desenvolvimento. **Quimica Nova**, v. 32, n. 7, p. 1971–1974, 2009.

DROR, O. et al. Novel approach for efficient pharmacophore-based virtual screening: method and applications. **J Chem Inf Model**, v. 49, n. 10, p. 2333–2343, 2009.

EHRLICH, P. Über den jetzigen Stand der Chemotherapie. **Berichte der deutschen chemischen Gesellschaft -Deutschen Chemischen Gesellschaft**, v. 42, n. 1, p. 17, 1909.

FRANÇA, T. C. C.; DOS SANTOS, M. G.; FIGUEROA-VILLAR, J. D. Malária: Aspectos históricos e quimioterapia. **Quimica Nova**, v. 31, n. 5, p. 1271–1278, 2008.

HASTINGS, I. M.; DONNELLY, M. J. The impact of antimalarial drug resistance mutations on parasite fitness, and its implications for the evolution of resistance. **Drug Resistance Updates**, v. 8, n. 1–2, p. 43–50, 2005.

HAWKINS, P. C. D. et al. Conformer Generation with OMEGA: Algorithm and Validation Using High Quality Structures from the Protein Databank and Cambridge Structural Database - Journal of Chemical Information and Modeling (ACS Publications). v. 11, p. 572–584, 2010.

HAWKINS, P.; SKILLMAN, A.; NICHOLLS, A. Comparison of Shape-Matching and Docking as Virtual Screening Tools. **Jornal of Medicial Chemistry**, v. 50, p. 74–82, 2007.

IRWIN, J.; SHOICHET, B. ZINC – A Free Database of Commercially Available Compounds for Virtual Screening. v. 45, n. 1, p. 177–182, 2005.

KIM, S. et al. PubChem substance and compound databases. **Nucleic Acids Research**, v. 44, n. D1, p. D1202–D1213, 2016.

LASKOWSKI, R. A.; SWINDELLS, M. B. LigPlot+: Multiple ligand-protein interaction diagrams for drug discovery. **Journal of Chemical Information and Modeling**, v. 51, n. 10, p. 2778–2786, 2011.

MCGANN, M. FRED pose prediction and virtual screening accuracy. **Journal of Chemical Information and Modeling**, v. 51, n. 3, p. 578–596, 2011.

MYSINGER, M. M. et al. Directory of useful decoys, enhanced (DUD-E): Better ligands and decoys for better benchmarking. **Journal of Medicinal Chemistry**, v. 55, n. 14, p. 6582–6594, 2012.

OOMS, F. Molecular modeling and computer aided drug design. Examples of their applications in medicinal chemistry. **Current medicinal chemistry**, v. 7, n. 2, p. 141–158, 2000.

PIRES, D. E. V.; BLUNDELL, T. L.; ASCHER, D. B. pkCSM: Predicting small-molecule pharmacokinetic and toxicity properties using graph-based signatures. **Journal of Medicinal Chemistry**, v. 58, n. 9, p. 4066–4072, 2015.

ROBERTS, C. W.; WALKER, W.; ALEXANDER, J. Sex-Associated Hormones and Immunity to Protozoan Parasites. **Clinical Microbiology Reviews**, v. 14, n. 3, p. 476–488, 2001.

RÓG, T. et al. Ordering effects of cholesterol and its analogues. **Biochimica et Biophysica Acta - Biomembranes**, v. 1788, n. 1, p. 97–121, 2009.

TATE, E. W. et al. Myristoyltransferase as a potential drug target in malaria and leishmaniasis. **Parasitology**, v. 141, n. 01, p. 37–49, 2014.

TOWLER, D. A. et al. Purification and characterization of yeast myristoyl CoA:protein N-myristoyltransferase. **Proceedings of the National Academy of Sciences of the United States of America**, v. 84, n. 9, p. 2708–2712, 1987.

VOM STEEG, L. G.; KLEIN, S. L. Sex Steroids Mediate Bidirectional Interactions Between Hosts and Microbes. **Hormones and Behavior**, v. 88, p. 45–51, 2017.

WERMUTH, C. G. et al. Glossary of Terms Used in medicinal Chemistry (IUPAC Recommendations). **Pure and Applied Chemistry**, v. 70, n. 5, p. 1129–1143, 1998.

WHO. **World Malaria Report 2017**. [s.l: s.n.].

WRIGHT, M. H. et al. Protein myristoylation in health and disease. **Journal of Chemical Biology**, v. 3, n. 1, p. 19–35, 2010.

WRIGHT, M. H. et al. Validation of N-myristoyltransferase as an antimalarial drug target using an integrated chemical biology approach. **Nature Chemistry**, v. 6, n. 2, p. 112–121, 2014.

YANG, S. H. et al. *N* -Myristoyltransferase 1 Is Essential in Early Mouse Development. **Journal of Biological Chemistry**, v. 280, n. 19, p. 18990–18995, 2005.

YU, Z. et al. Design and Synthesis of Inhibitors of *Plasmodium falciparumN* -Myristoyltransferase, A Promising Target for Antimalarial Drug Discovery. **Journal of Medicinal Chemistry**, v. 55, n. 20, p. 8879–8890, 2012.

ZHAO, C.; MA, S. Recent Advances in The Discovery of N-Myristoyltransferase Inhibitors. **ChemMedChem**, v. 9, n. 11, p. 1–14, 2014.

ZOETE, V. et al. SwissParam: A Fast Force Field Generation Tool for Small Organic Molecules. **Wiley Online Library**, 2011.